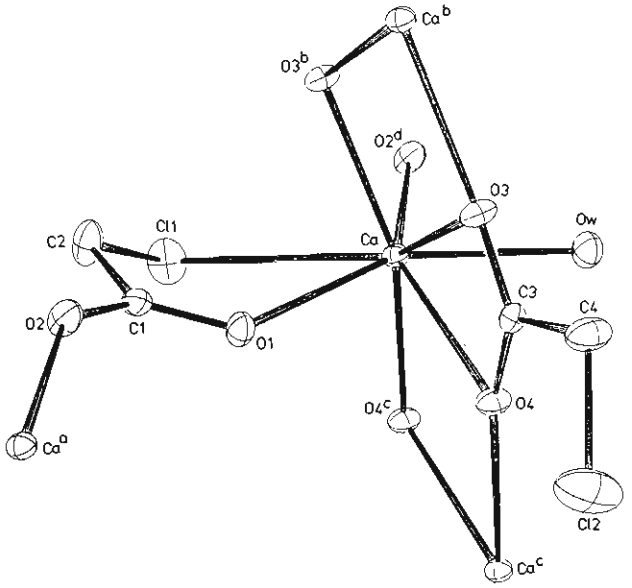

Figure 1. A portion of the crystalline structure showing the mode of chloroacetate–Ca^{2+} binding and the atom-labeling scheme. Hydrogen atoms have been omitted for clarity. Chloroacetate (A) is specified by atoms O(1), O(2), C(1), C(2), Cl(1) and chloroacetate (B) by atoms O(3), O(4), C(3), C(4), Cl(2). The superscripts specify the symmetry-related positions of the atoms given in Table I: (a) $x - 1, y, z$; (b) $-x, -y, 2 - z$; (c) $-x, -y, 1 - z$; (d) $x + 1, y, z$.

Hydrogen atom parameters were not refined. The function minimized in the least-squares procedure was $\sum w(|F_o| - |F_c|)^2$, where $w = [(\sigma(F_o))^2 + (0.02F_o)^2]^{-1}$. Anisotropic refinement (on F) of all non-hydrogen atoms (109 variable parameters; 15.3 data/parameter) converged to a conventional R factor (R) of 0.046, a weighted R factor (R_w) of 0.055, and an error in an observation of unit weight of 1.62. In the final cycle of refinement the largest ratio of shifts to estimated standard deviations was 0.01. Final fractional coordinates and equivalent isotropic thermal parameters are given in Table I.

Results and Discussion

There are no symmetry conditions imposed on the crystalline structure by the space group, and the asymmetric unit consists of one Ca^{2+}, two independent chloroacetate ions (designated A and B), and one water molecule. A view of the structure is shown in Figure 1. Bond distances and angles are given in Table II.

The most significant feature revealed in this structural investigation is the direct participation of a carbon-bound chlorine atom in Ca^{2+} binding. The two chloroacetate ligands differ in the manner in which they coordinate Ca^{2+} ions. Chloroacetate (A) chelates a Ca^{2+} ion through its chlorine atom, Cl(1), and carboxylate oxygen, O(1), forming a buckled five-membered chelate ring. In addition, a second Ca^{2+} ion is coordinated to carboxylate (A) oxygen, O(2), via a unidentate bridging interaction. Chloroacetate (B) binds three different Ca^{2+} ions through its carboxylate group—one through a reasonably symmetric, planar four-membered chelate ring and two others through unidentate bridging bonds, which lead to the formation of planar Ca–O–Ca–O four-membered rings. These bridging interactions are common features[7] in calcium carboxylates and form the basis for the polymeric nature of the crystalline structure.

This C–Cl···Ca^{2+} binding is to the best of our knowledge the first example of direct Ca^{2+}–halocarbon binding. An example of indirect Ca^{2+}–fluorocarbon binding mediated through a coordinated water molecule has been recently described.[2] The Ca^{2+}–Cl(1) distance is 3.206 (1) Å, which is in the range expected for a weak ion–dipole C–Cl···Ca^{2+} interaction. Essentially full ionic Ca^{2+}···Cl^- separations (2.741 Å in $CaCl_2 \cdot 4H_2O$)[8] are, of course, considerably shorter. Although there are no other reported direct chlorocarbon–Ca^{2+} linkages, the observed distance is shorter than the comparable C–Cl···K^+ separations (range 3.243–3.462 Å) found in potassium hydrogen chloromaleate,[9] potassium hydrogen trichloroacetate,[10] potassium hydrogen dichloroacetate,[11] and potassium bis(chloroacetato)stannate(II).[12]

The intramolecular bond lengths and angles of the two independent chloroacetate groups (Table I) are similar to the dimensions reported in other structures containing chloroacetate.[12-17] The dihedral angles between the carboxylate plane and the corresponding C–C–Cl plane are 18.8 and 25.4° for chloroacetate (A) and chloroacetate (B), respectively.

The CaO_7Cl polyhedron deviates extensively from idealized eight-coordinate geometries, and selection of an appropriate stereochemical description for eight-coordinate polyhedra is often difficult.[18] An analysis of shape parameters suggests the CaO_7Cl polyhedron lies along the reaction pathway connecting a dodecahedron and bicapped trigonal prism.[19]

Calcium chloroacetate monohydrate is easily crystallized from aqueous solution, and in view of the high affinity of Ca^{2+} for oxygen donor groups, it appears remarkable that the carbon-bound chlorine effectively competes with carboxylate oxygens and water molecules for Ca^{2+} binding. Because chloroacetate is well-known to bind metal ions only through its carboxylate group, the C–Cl···Ca^{2+} interaction does not arise because of any inherent geometrical constraint imposed by the ligand or complex. Thus, although weak, the observed C–Cl···Ca^{2+} binding represents a genuine attractive interaction that is undoubtedly largely Coulombic in origin. Although direct evidence is lacking, this C–Cl···Ca^{2+} binding may probably even occur in solution (albeit fleeting) inasmuch as this interaction survives in the crystal.

Acknowledgment. We are grateful to the National Science Foundation for a grant (CHE-8418897) (A.K.) used to purchase the CAD4 X-ray diffractometer system.

Registry No. $Ca(CH_2ClCOO)_2(H_2O)$, 72134-84-0.

Supplementary Material Available: Tables S1 and S2, listing anisotropic displacement parameters and hydrogen-bonding parameters (2 pages); table of calculated and observed structure factors (8 pages). Ordering information is given on any current masthead page.

(7) Einspahr, H.; Bugg, C. E. *Acta Crystallogr., Sect. B: Struct. Crystallogr. Cryst. Chem.* **1981**, *B37*, 1044.
(8) Leclair, A.; Borel, M. M.; Monier, J. C. *Acta Crystallogr., Sect. B: Struct. Crystallogr. Cryst. Chem.* **1980**, *B36*, 2757.
(9) Ellison, R. D.; Levy, H. A. *Acta Crystallogr.* **1965**, *19*, 260.
(10) Golic, L.; Lazarini, F.; *Cryst. Struct. Commun.* **1974**, *3*, 645.
(11) Hadzi, D.; Leban, I.; Orel, B.; Iwata, M.; Williams, J. M. *J. Cryst. Mol. Struct.* **1979**, *9*, 117.
(12) Clark, S. J.; Donaldson, J. D.; Dewar, J. C.; Silver, J. *Acta Crystallogr., Sect. B: Struct. Crystallogr. Cryst. Chem.* **1979**, *B35*, 2550.
(13) Solans, X.; Miravitlles, C. *Acta Crystallogr., Sect. B: Struct. Crystallogr. Cryst. Chem.* **1981**, *B37*, 1407.
(14) Dewan, J. C. *Acta Crystallogr., Sect. B: Struct. Crystallogr. Cryst. Chem.* **1980**, *B36*, 1935.
(15) Faggiani, R.; Johnson, J. P.; Brown, I. D.; Birchall, T. *Acta Crystallogr., Sect. B: Struct. Crystallogr. Cryst. Chem.* **1978**, *B34*, 3742.
(16) Ichikawa, M. *Acta Crystallogr., Sect. B: Struct. Crystallogr. Cryst. Chem.* **1978**, *B28*, 755.
(17) (a) Davey, G.; Stephens, F. S. *J. Chem. Soc. A* **1971**, 1917. (b) Davey, G.; Stephens, F. S. *J. Chem. Soc. A* **1970**, 2803.
(18) Burdett, J. K.; Hoffman, R.; Fay, R. C. *Inorg. Chem.* **1978**, *17*, 2553.
(19) (a) Mutterties, E. L.; Guggenberger, L. J. *J. Am. Chem. Soc.* **1974**, *96*, 1748. (b) Kouba, J. K.; Wreford, S. S. *Inorg. Chem.* **1976**, *15*, 1463.

Contribution from the Rosenstiel School of Marine and Atmospheric Science, University of Miami, 4600 Rickenbacker Causeway, Miami, Florida 33149

Determining the Stability Constant of Copper(I) Halide Complexes from Kinetic Measurements

Virender K. Sharma and Frank J. Millero*

Received March 15, 1988

Copper in oxidation state I seems to be the only first-row transition element showing typical class B behavior, characterized by the halide affinity sequence $F^- \ll Cl^- < Br^- < I^-$ in aqueous solution.[1,2] The complex formation of an acceptor in such a unique

Table I. Rate Constants (mol^{-1} kg min^{-1}) Measured in $NaX-NaClO_4$ Mixtures (X = Cl^-, Br^-, I^-) at I = 1, pH 8, and 25 °C

	log k		
[X^-], M	Cl^-	Br^-	I^-
0.05			4.18
0.10			3.74
0.15		4.07	
0.20		3.84	
0.30		3.49	2.96
0.40	4.22	3.18	
0.50	4.01	2.98	2.30
0.60	3.92	2.73	
0.70	3.76	2.50	2.16
0.85		2.36	
0.90	3.52		
1.00	3.43	2.16	1.84

position is of special interest. The hydrated copper(I) ion disproportionates almost completely, except at extremely low concentrations. Copper(I) is, therefore, stable in the presence of ligands forming strong complexes. All halide ions with the exception of the fluoride ion belong to this group.[3] Their complex formation has in fact been studied since the beginning of the century,[4] but due to the severe experimental difficulties, many points have nevertheless remained obscure.

Most attempts to determine stability constants have been made by using either solubility or electromotive force data at constant ionic strength.[2,5-9] In all of these attempts, the lower limit of the ligand concentration is set by the low stability of the neutral complexes. As soon as these constitute an appreciable part of the copper(I) present in the solution, the total solubility becomes too low for potentiometric measurements. Even when solubility measurements are used, solutions containing much of the copper(I) as CuX (X = Cl^-, Br^-, I^-) are difficult to obtain. On account of these experimental difficulties, the stability constant for formation of $Cu^+ + I^- \rightleftharpoons CuI^0$ is unknown in the literature.

In the present work, we have studied the oxidation of Cu(I) with molecular oxygen in $NaX-NaClO_4$ mixtures (X = Cl^-, Br^-, I^-) at ionic strength I = 1 and at 25 °C. The stability constant of CuI^0 is determined by using kinetic results and known values of the stability constants for $CuCl^0$ [2] and $CuBr^0$.[9]

Experimental Section

The oxidation reactions were carried out in a 500-cm^3 water-jacketed cell. The temperature of the cell was controlled to ±0.02 °C with a Forma bath. The top of the cell was fitted with a glass frit used to bubble air through the solutions and an autopipet was used to remove sample aliquots during a run.

The Cu(I) concentrations during a run were determined spectrophotometrically by using bathocuproine (2,9-dimethyl-4,7-diphenyl-1,10-phenanthroline) and the method developed by Moffett et al.[10] The absorbance of the solution was measured at 484 nm with a Varian Cary 2200 UV–vis spectrophotometer. All measurements were made at micromolar levels of Cu(I). EDTA (10^{-5} M) was added[10] to prevent the back-reaction of Cu(II).

Stock solutions of Cu(I) were prepared fresh daily by a method described elsewhere.[10] The $NaX-NaClO_4$ (X = Cl^-, Br^-, I^-) solutions were made by using reagent grade chemicals and Millipore Super Q ion-exchanged water (18 MΩ).

The solutions were buffered by using 10^{-3} M borate. Tris (0.005 m) buffers in NaCl were used to determine pH and to calibrate electrode systems. The calibrations were made on the pH scale of Millero et al.[11]

All of the measurements were made in solutions saturated with air at a given temperature by bubbling. The molal concentrations of O_2 in the solutions at a given temperature and ionic strength were determined by using the pure water solubility results of Benson and Krause[12] and salting coefficient k = 0.132[13] for NaCl solutions.

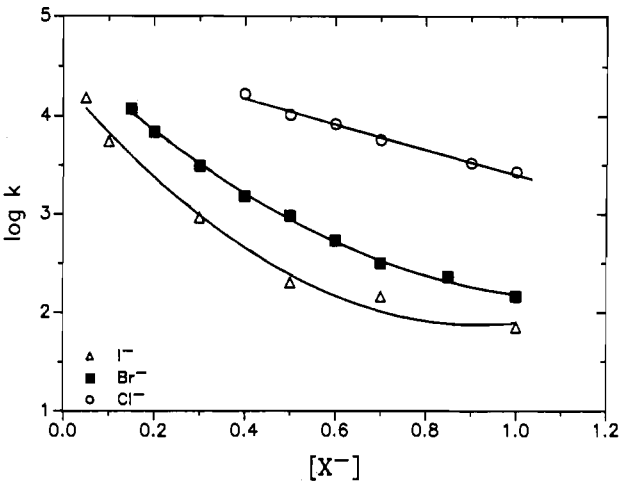

Figure 1. log k vs [X^-] for the oxidation of Cu(I) in $NaX-NaClO_4$ solutions at I = 1 and 25 °C (X = Cl^-, Br^-, I^-).

Table II. β_i^* Values for Copper(I) Halide Species at 25 °C and I = 1

	log β_1^*	log β_2^*	log β_3^*	ref
chloride	2.71[a]	5.06	4.97	8
bromide	3.15	5.41	6.65	9
iodide		8.13	9.46	6

[a] Reference 2.

Results and Discussion

The rate constant (k, kg mol^{-1} min^{-1}) for the oxidation of Cu(I)

$$d[Cu(I)]/dt = -k[Cu(I)][O_2] \quad (1)$$

has been determined in $NaX-NaClO_4$ (X = Cl^-, Br^- I^-) mixtures at ionic strength I = 1, pH 8, and 25 °C. The results are given in Table I and shown versus [X^-] in Figure 1. The decrease in the rate constants is as expected ($Cl^- > Br^- > I^-$) due to expected stability of Cu^+ complexes.

The oxidation of various ion-paired forms of copper(I) halide complexes can be attributed to[14]

$$Cu^+ + O_2 \xrightarrow{k_0} \text{products} \quad (2)$$

$$CuX^0 + O_2 \xrightarrow{k_1} \text{products} \quad (3)$$

$$CuX_2^- + O_2 \xrightarrow{k_2} \text{products} \quad (4)$$

$$CuX_3^{2-} + O_2 \xrightarrow{k_3} \text{products} \quad (5)$$

The measured rate constant is related to the individual value by

$$k[Cu]_T = k_0[Cu]_F + k_1[CuX] + k_2[CuX_2] + k_3[CuX_3] \quad (6)$$

which can be simplified to

$$k = k_0\alpha_{Cu} + k_1\alpha_{CuX} + k_2\alpha_{CuX_2} + k_3\alpha_{CuX_3} \quad (7)$$

(1) Ahrland, S.; Chatt, J.; Davies, N. R. *Chem. Rev.* **1958**, *12*, 265.
(2) Ahrland, S.; Rawthorne, J. *Acta Chem. Scand.* **1970**, *24*, 157.
(3) Latimer, W. M. *The Oxidation States of the Elements and Their Properties in Aqueous Solutions*, 2nd ed.; Prentice-Hall: Englewood Cliffs, NJ, 1952; p 183.
(4) Bodlander, G.; Storbeck, P. Z. *Z. Anorg. Chem.* **1902**, *31*, 458.
(5) Peters, D. G.; Caldwell, R. L. *Inorg. Chem.* **1967**, *6*, 1478.
(6) Ahrland, S.; Tagerson, B. *Acta Chem. Scand., Ser. A* **1977**, *A31*, 615.
(7) Fritz, J. J. *J. Phys. Chem.* **1981**, *85*, 890.
(8) Fritz, J. J. *J. Phys. Chem.* **1984**, *88*, 4358.
(9) Fritz, J. J.; Luzik, E. *J. Soln. Chem.* **1987**, *16*, 79.
(10) Moffett, J. W.; Zika, R. G.; Petasne, R. G. *Anal. Chim. Acta* **1985**, *175*, 171.
(11) Millero, F. J.; Hershey, J. P.; Fernandez, M. *Geochim. Cosmochim. Acta* **1987**, *51*, 707.
(12) Benson, R. B.; Krause, D., Jr. *Limnol. Oceanogr.* **1986**, *29*, 620.
(13) Harned, H. S.; Owen, B. B. *The Physical Chemistry of Electrolyte Solutions*; ACS Monograph 137; Reinhold: New York, 1958; p 803.
(14) Millero, F. J. *Geochim. Cosmochim. Acta* **1985**, *49*, 547.

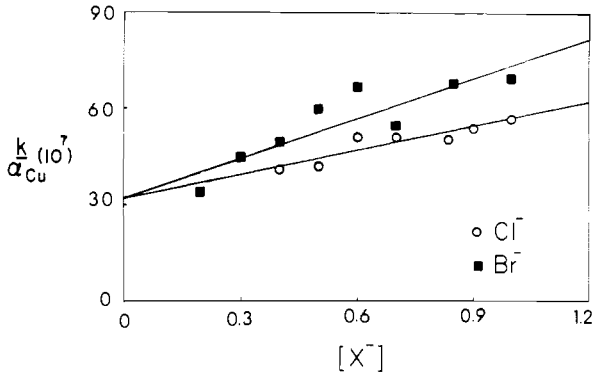

Figure 2. k/α_{Cu} vs $[X^-]$ for the oxidation of Cu(I) in NaX–$NaClO_4$ solutions at I = 1 and 25 °C (X = Cl^-, Br^-).

Table III. Rate Constants for the Oxidation of Cu^+ and CuX^0 (X = Cl^-, Br^-, I^-) at I = 1, pH 8, and 25 °C

	log β_1*	log k_0	log k_1
chloride	2.71[a]	8.47 ± 0.03	5.68 ± 0.08
bromide	3.15[b]	8.45 ± 0.09	5.56 ± 0.06
iodide	5.7 ± 0.7	8.46 ± 0.02[c]	5.62 ± 0.25[c]

[a] Reference 2. [b] Reference 9. [c] Average values for Cl^- and Br^- solutions.

where molar fraction α_i of the various species can be estimated from

$$\alpha_{Cu} = [1 + \beta_1^*[X^-] + \beta_2^*[X^-]^2 + \beta_3^*[X^-]^3]^{-1} \quad (8)$$

$$\alpha_{CuX} = \beta_1^*[X^-]\alpha_{Cu} \quad (9)$$

$$\alpha_{CuX_2} = \beta_2^*[X^-]^2\alpha_{Cu} \quad (10)$$

$$\alpha_{CuX_3} = \beta_3^*[X^-]^3\alpha_{Cu} \quad (11)$$

The substitution into equation 7 gives

$$k/\alpha_{Cu} = k_0 + k_1\beta_1^*[X^-] + k_2\beta_2^*[X^-]^2 + k_3\beta_3^*[X^-]^3 \quad (12)$$

The values of β_i^* at I = 1 are given in Table II. We have extrapolated the values of Fritz[9] at infinite dilution to I = 1 using Pitzer's equation,[15] assuming $\gamma_{Cu} = \gamma_{Na}$ and $\ln \gamma_{CuX} = 0.132I$.[16] We have also extrapolated the values of Ahrland and Tagerson[6] in sodium iodide solutions from I = 5 to I = 1.

The plots of k/α_{Cu} for Cl^- and Br^- ions are given in Figure 2. The plots show a linear relationship for both Cl^- and Br^- ions. Therefore, eq 12 becomes

$$k/\alpha_{Cu} = k_0 + k_1\beta_1^*[X^-] \quad (13)$$

The values extrapolated to pure-water conditions (k_0 = (3 ± 0.2) × 10^8 mol^{-1} kg min^{-1}) are the same for both Cl^- and Br^- ions within experimental error. The values of k_1 for the oxidation of $CuCl^0$ and $CuBr^0$ complexes (Table III) are also the same within experimental error. These results indicate that rates of oxidation for CuX (X = Cl^-, Br^-) are not influenced by the nature of the ligand.

It is not possible to make similar calculations for the NaI mixtures because β_1^* is not known. If we assume that k_1 for the oxidation of CuI^0 averages 4.2 × 10^5 mol^{-1} kg min^{-1}, it is possible to estimate the value of β_1^* from the kinetic data. We have made this estimate by first assuming that $\beta_1^*[X^-]$ does not contribute to α_{Cu}. This assumption is well justified at $[X^-]$ = 1.0 M but causes errors in α_{Cu} at low concentrations of X^-. This gives a first approximation of k/α_{Cu}, which is plotted versus $[I^-]$. Since the intercept (k_0) of eq 13 in NaI solutions must be the same as those for NaCl and NaBr, the slope can be first estimated from the value of k/α_{Cu} at $[X^-]$ = 1.0 M. This slope can be used to make an estimate of β_1^*

$$\beta_1^* = [(k/\alpha_{Cu}) - k_0]/k_1 \quad (14)$$

(15) Pitzer, K. S.; Mayorga, G. *J. Phys. Chem.* **1973**, *77*, 2300.
(16) Millero, F. J. Schreiber, D. R. *Am. J. Sci.* **1982**, *282*, 1508.

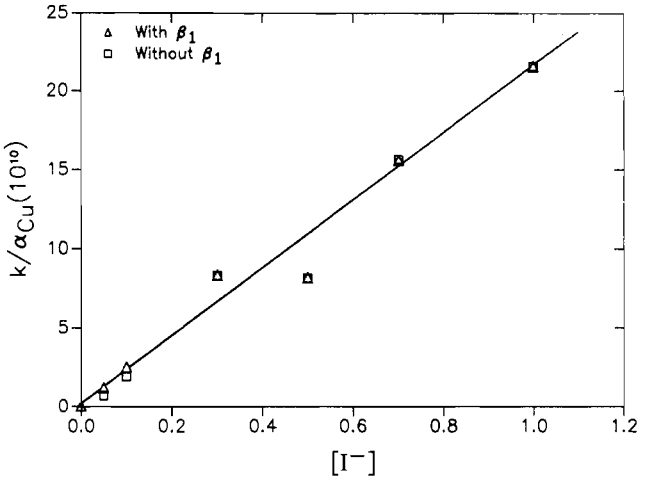

Figure 3. k/α_{Cu} vs $[I^-]$ for the oxidation of Cu(I) in NaX–$NaClO_4$ at I = 1 and 25 °C (X = Cl^-, Br^-, I^-).

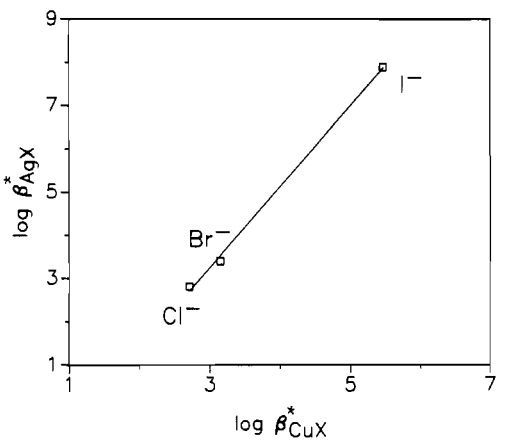

Figure 4. log β^*_{AgX} vs log β^*_{CuX} at I = 1 and 25 °C (X = Cl^-, Br^-, I^-).

This estimated β_1^* (log β_1^* = 5.69) is then used to determine the values of k/α_{Cu} over the entire concentration range (Figure 3). The new slope is determined by a least-squares fit and gives a new value of β_1^*. The process is repeated until a self-consistent value of log β_1^* = 5.7 ± 0.7 is obtained. Since the $\beta_1[X^-]$ term does not signifificantly contribute to α_{Cu} over the concentration range of our kinetic measurements, the initial estimate of β_1^* is equal within experimental error to the first estimate. This estimated value agrees with the expected trend in stability constants ($CuCl^0$ < $CuBr^0$ < CuI^0).

This trend in stability constants ($CuCl^0$ < $CuBr^0$ < CuI^0) is to be expected for interactions taking place in aqueous solutions between the soft metal ions Cu(I) and the heavy halides, the softness of which increases in the order mentioned. This is because the bonds are markedly covalent, and the covalent character is strengthened as the ligand becomes softer.

The data for copper(I)–halide complexes are compared with those for silver(I) halide systems because Ag(I) has the same electronic configuration, d^{10}. Silver(I) halide complexes show a similar trend in stability constants, Cl^- < Br^- < I^-;[6] however, Ag(I) forms a stronger complex than does Cu(I).[17-19] This is shown in Figure 4, in which the slope of log β^*_{AgX} vs log β^*_{CuX} has a value greater than 1. This is as expected because of the stronger class B character of Ag(I) due to its position in a higher period.

In summary, it has been clearly shown that kinetic results can be used to determine stability constants of copper(I) halide complexes, which are otherwise difficult to determine by either sol-

(17) Fritz, J. J. *J. Soln. Chem.* **1985**, *14*, 865.
(18) Berne, E.; Leden, I. *Z. Naturforsch., A: Astrophys., Phys., Phys. Chem.* **1953**, *8A*, 719.
(19) Leden, I. *Acta Chem. Scand.* **1956**, 812.

ubility or potentiometric methods. The resulting estimate for the stability constant of CuI is as expected for the class B metals and correlates very well with the value for AgI.

Acknowledgment. We wish to acknowledge the support of the Office of Naval Research (Grant N00014-87-G0116) and the oceanographic section of the National Science Foundation (Grant OCE86-00284) for this study.

Registry No. Cu, 7440-50-8.

Contribution from the Department of Chemistry and James Franck Institute, The University of Chicago, Chicago, Illinois 60637

Band Gap and Stability of Solids

Jeremy K. Burdett,* Barry A. Coddens, and Gururaj V. Kulkarni

Received March 4, 1988

The presence of a good HOMO–LUMO gap in molecules has long been associated with structural and kinetic stability. Bartell's use of the second-order Jahn–Teller theorem highlighted this viewpoint when he showed how molecules with small gaps could distort to give more stable structures with larger gaps.[1] An example is the opening up of the gap on pyramidalization of ammonia. In studying the most stable substitution pattern of cyclobutadienes, Hoffmann identified the more stable (trans) $A_2B_2C_4$ isomer as the one with the larger HOMO–LUMO gap.[2] In organometallic chemistry as well, similar ideas apply. Whether the cis or trans form of $ML_4(CO)_2$ and ML_4O_2 species is more stable depends upon electron count. However, in each case for a given electron configuration the more stable structure is found to be the one with the larger gap. In fact, the concept that a small HOMO–LUMO gap signals a geometric distortion is well recognized in almost all areas of molecular chemistry. Notice that in all these examples the number and type of internuclear contact remain the same within each pair of examples. It is either the way the atoms are connected or the angles associated with pairs of bonds that change. In terms of the language of the method of moments, which we have used[3–6] extensively to study structural–electronic problems, the second moment of the electronic density of states remains invariant. There is, however, a less well established view that a correlation analogous to the one described above for molecules applies to solids. In this paper we show the formal connection between stability and band gap in solids by using a simple model that reproduces the results obtained via band structure computations. The model is easily transferable to molecules.

Gaps and Stability in Solids

In molecules the concept of isomerism is well established. The cis- and trans-substituted cyclobutadienes and transition-metal complexes mentioned above are a good example. In solids their equivalent is perhaps the possibility of "coloring" patterns of atoms over the sites of a given lattice.[3] The ZnS (sphalerite) structure may be described in several different ways. One route generates the structure by filling with Zn atoms all the upward-pointing tetrahedral holes of the cubic anion close-packing. A complementary pathway generates the structure by filling with S atoms all the upward-pointing tetrahedral holes of the cubic cation close-packing. In the derivative A_2XX' arrangement there can then be a variety of ways of ordering the X and X′ atoms over the S sites of either description. **1** and **2** show two possibilities.

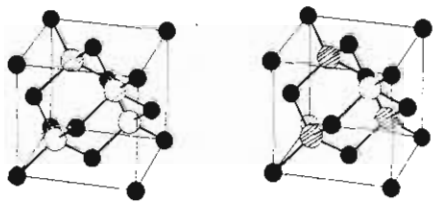

1 **2**

sphalerite : Zn, P, S

Similarly, although the simple cubic structure is made up of three mutually perpendicular strings of atoms and can be viewed as a degenerate rock salt structure, there are other ways of ordering the Na and Cl atoms over the lattice. **3** and **4** show two possibilities for two different metal ions ordered over the octahedral hole of a close packing of halogen atoms. Table I shows the computed band gaps (E_g) and stabilities (ΔE) of four pairs of examples. The band structure calculations use the extended Hückel implementation of the tight-binding type method. The examples of Table I include the colorings of sphalerite and rock salt just described. The spinel structure (AB_2X_4) may be regarded as a rock salt/sphalerite hybrid in the sense that both octahedral and tetrahedral holes of the close packing are partially occupied. One of the examples of Table I compares the energies of two colorings (**5** and **6**) of the spinel structure. Coloring patterns do not always have to involve atoms; they can just as well involve vacancies. Thus, the final pair of examples (**7** and **8**) are two

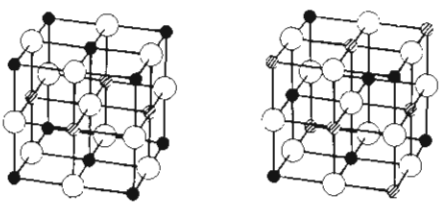

3 **4**

rock salt : P, Mg, Zr

Table I. Computed Band Gaps and Relative Stabilities for Different Ordering Patterns in Simple Solids

system	stoichiometry[b]	coordn environment	ΔE, eV[a]	E_g, eV
sphalerite	A_2XX'	2 + 2 (cation)	0	1.8
		3 + 1, 1 + 3 (cation)	0.3	1.5
rock salt	$AA'X_2$	3 + 3 (anion)	0	3.05
		4 + 2, 2 + 4 (anion)	0.5	2.40
defect ReO_3	$AX_{2.5}$	5[c] (cation)	0	2.84
		5[c] (cation)	0.2	2.80
spinel	$AA'_2X_2X'_2$	2 + 4 (cation A′), 2 + 2(A)	0	1.17
		3 + 3 (cation A′), 4 + 0(A)	0.17	1.15

[a] The most stable structure has $\Delta E = 0$. [b] In sphalerite the coloring is of P and S atoms in a fixed lattice of Zn, in rock salt it is of Mg and Zr atoms in a lattice of P atoms, in the ReO_3 structure it is of oxygen over an array of a prototypic transition metal (Mn parameters were used), and in the spinel it is of Mg and Sc over a close-packed array of P and S atoms. The details of the structures are shown in **1–6**. (Geometric details and orbital parameters are given in the Appendix.) [c] In these structures there are two different ordering patterns for the AX_5 square pyramids (see **7** and **8**).

(1) Bartell, L. S. *J. Chem. Educ.* **1968**, *45*, 754.
(2) Hoffmann, R. *J. Chem. Soc., Chem. Commun.* **1979**, 240.
(3) Burdett, J. K.; Lee, S.; McLarnan, T. J. *J. Am. Chem. Soc.* **1985**, *107*, 3083.
(4) Burdett, J. K.; Lee, S. *J. Am. Chem. Soc.* **1985**, *107*, 3050.
(5) Burdett, J. K.; Lee, S. *J. Am. Chem. Soc.* **1985**, *107*, 3063.
(6) Burdett, J. K. *Struct. Bonding (Berlin)* **1987**, *65*, 30.

0020-1669/88/1327-3259$01.50/0